NAMPT-mediated NAD+ biosynthesis is indispensable for adipose tissue plasticity and development of obesity

Nielsen, Karen Nørgaard; Peics, Julia; Ma, Tao; Karavaeva, Iuliia; Dall, Morten; Chubanava, Sabina; Basse, Astrid L; Dmytriyeva, Oksana; Treebak, Jonas T; Gerhart-Hines, Zachary

MOLECULAR
METABOLISM

NAMPT-mediated NAD$^+$ biosynthesis is indispensable for adipose tissue plasticity and development of obesity

Karen Nørgaard Nielsen [1,2,6], Julia Peics [1,6], Tao Ma [1,2,6], Iuliia Karavaeva [1,2], Morten Dall [3],
Sabina Chubanava [3], Astrid L. Basse [3], Oksana Dmytriyeva [4,5], Jonas T. Treebak [3], Zachary Gerhart-Hines [1,2,*]

ABSTRACT

Objective: The ability of adipose tissue to expand and contract in response to fluctuations in nutrient availability is essential for the maintenance of whole-body metabolic homeostasis. Given the nutrient scarcity that mammals faced for millions of years, programs involved in this adipose plasticity were likely evolved to be highly efficient in promoting lipid storage. Ironically, this previously advantageous feature may now represent a metabolic liability given the caloric excess of modern society. We speculate that nicotinamide adenine dinucleotide (NAD$^+$) biosynthesis exemplifies this concept. Indeed NAD$^+$/NADH metabolism in fat tissue has been previously linked with obesity, yet whether it plays a causal role in diet-induced adiposity is unknown. Here we investigated how the NAD$^+$ biosynthetic enzyme nicotinamide phosphoribosyltransferase (NAMPT) supports adipose plasticity and the pathological progression to obesity.

Methods: We utilized a newly generated *Nampt* loss-of-function model to investigate the tissue-specific and systemic metabolic consequences of adipose NAD$^+$ deficiency. Energy expenditure, glycemic control, tissue structure, and gene expression were assessed in the contexts of a high dietary fat burden as well as the transition back to normal chow diet.

Results: Fat-specific *Nampt* knockout (FANKO) mice were completely resistant to high fat diet (HFD)-induced obesity. This was driven in part by reduced food intake. Furthermore, HFD-fed FANKO mice were unable to undergo healthy expansion of adipose tissue mass, and adipose depots were rendered fibrotic with markedly reduced mitochondrial respiratory capacity. Yet, surprisingly, HFD-fed FANKO mice exhibited improved glucose tolerance compared to control littermates. Removing the HFD burden largely reversed adipose fibrosis and dysfunction in FANKO animals whereas the improved glucose tolerance persisted.

Conclusions: These findings indicate that adipose NAMPT plays an essential role in handling dietary lipid to modulate fat tissue plasticity, food intake, and systemic glucose homeostasis.

© 2018 The Authors. Published by Elsevier GmbH. This is an open access article under the CC BY-NC-ND license (http://creativecommons.org/licenses/by-nc-nd/4.0/).

Keywords Adipose metabolism; Obesity; NAMPT; NAD$^+$ synthesis; Energy homeostasis; Adipose plasticity; Glucose homeostasis

1. INTRODUCTION

The efficient storage of dietary calories in adipose tissue is a key evolutionary advantage honed over millions of years of nutrient scarcity [1,2]. However, societal advances in the past century have made cheap, calorie-dense foodstuffs readily available. As a result, some bioenergetic programs that were once beneficial for survival may now pose a disadvantage in the context of metabolic disease [1–3]. Under

normal, healthy conditions, adipose tissue exhibits a remarkable plasticity and can dynamically accumulate or release lipid stores depending on nutrient availability and hormonal signaling [4–6]. This expansion is accomplished through increases in both fat cell number and size [7] and remodeling of non-adipocyte tissue features such as vasculature and extracellular matrix [6,8]. However, sustained caloric excess disrupts this energy balance leading to tissue inflammation, insulin resistance, and, ultimately, systemic metabolic dysfunction

[1]Section for Metabolic Receptology, Novo Nordisk Foundation Center for Basic Metabolic Research, University of Copenhagen, 2200 Copenhagen, Denmark [2]Department of Biomedical Sciences, University of Copenhagen, 2200 Copenhagen, Denmark [3]Section for Integrative Physiology, Novo Nordisk Foundation Center for Basic Metabolic Research, University of Copenhagen, 2200 Copenhagen, Denmark [4]Laboratory of Neural Plasticity, Institute of Neuroscience, University of Copenhagen, 2200 Copenhagen, Denmark [5]Research Laboratory for Stereology and Neuroscience, Bispebjerg-Frederiksberg Hospital, Copenhagen University Hospital, 2400 Copenhagen, Denmark

[6] Co-first authors.

*Corresponding author. Section for Metabolic Receptology, Novo Nordisk Foundation Center for Basic Metabolic Research, University of Copenhagen, Blegdamsvej 3B, 7.6.56, 2200 Copenhagen, Denmark. E-mail: zpg@sund.ku.dk (Z. Gerhart-Hines).

[5,6]. Understanding the fundamental systems that govern adipocyte lipid accumulation versus lipolysis and oxidation could provide valuable therapeutic insight [9].

An evolutionarily advantageous program fine-tuned to maximize fat accumulation would be most induced under times of nutrient scarcity to ensure efficient storage and survival. Conversely, during periods of caloric excess in which such a system would be superfluous, we predicted that this program would be decreased. Interestingly, the expression of the nicotinamide adenine dinucleotide (NAD^+) biosynthetic enzyme Nicotinamide phosphoribosyltransferase (NAMPT) mirrors such a pattern. In mice, adipose *Nampt* expression has been found to be decreased in response to high fat diet (HFD) [10,11] and induced by caloric restriction [12]. In fact, chemical inhibition of NAMPT has been shown to abolish the beneficial effects of caloric restriction [13]. NAMPT acts intracellularly to catalyze the rate-limiting step of the NAD^+ salvage pathway [14], the main source of adipose NAD^+ [15], but can also be secreted extracellularly as an adipokine [15,16]. Both functions of NAMPT appear to contribute to peripheral [17] and central [15] control of murine systemic metabolic homeostasis.

In humans, visceral adipose *NAMPT* expression and serum NAMPT levels are positively correlated with several metrics of obesity [18—21]. Conversely, *NAMPT* levels in subcutaneous adipose appear to be lower in obese subjects [22—24]. These divergent patterns of *NAMPT* association suggest differing depot-specific NAMPT contributions in human fat and make it difficult to assign a positive or negative role of NAMPT in metabolic syndrome. Human genetic studies have provided little clarity. Whereas *NAMPT* genetic variation was associated with increased obesity prevalence in a cohort of Indian children [25], another study identified a *NAMPT* variant that was associated with protection from severe obesity in a French population [26]. These previous clinical and genetic studies focused primarily on understanding the correlative links between adipose *NAMPT* and metabolic disease parameters. Here we now seek to determine whether NAMPT plays a causal role in adipose tissue dynamics and the development of obesity.

2. EXPERIMENTAL PROCEDURES

2.1. Animals

The $Nampt^{f/f}$ mouse model was generated by flanking exon 3 of the *Nampt* gene with loxP sites [27]. This line was continuously backcrossed to the C57BL/6JBomTac background. Female $Nampt^{f/f}$ mice were mated with male *Adiponectin*-Cre mice [28] (010803, Jackson Labs), kindly provided by Prof. Karsten Kristiansen. Expression of a functional pan-adipose Cre recombinase in the floxed model results in loss of function of the *Nampt* gene in all adipose depots by deleting exon 3 and by introducing a downstream frameshift and a premature stop codon in exon 4. Experimental cohorts were bred using female $Nampt^{f/f}$ mice mated with male $Nampt^{f/f}$, heterozygote Cre^+ mice. All experiments were conducted in male mice, and $Nampt^{f/f}$, Cre^- mice were used as controls. A minimum of six mice was included in each experimental group.

Mice were housed on a 12:12 h light/dark cycle (lights on at 6am, off at 6pm) at room temperature (22 °C) in an enriched environment with ad libitum access to water and chow diet (1310, Altromin). High fat diet feeding (D12492, Research Diets) was initiated in 12-20-week-old mice. Mice were generally group housed but were singly housed for indirect calorimetry experiments. Whole body composition was determined by quantitative magnetic resonance (MR) using an Echo-MRI™-4in1 Body Composition Analyzer (EchoMRI).

All animal experiments were conducted in accordance with the Danish Animal Research authorities under license no. 2014-15-0201-00181.

2.2. Indirect calorimetry

Indirect calorimetry was performed using the Phenomaster Home Cage System (TSE Systems). Briefly, animals were acclimated in training cages for 3—5 days prior to the measurement. All data were recorded in 5-minute intervals. Temperature and activity monitoring was conducted using implanted E-Mitters described below. Data collection was integrated into the TSE software. RER is depicted as rolling averages of five data points. Energy expenditure is presented as raw values plotted against either body weight or lean mass.

2.3. Telemetry

Temperature and gross motor activity was measured using G2 E-Mitters and ER4000 Energizer/Receiver (STARR Life Sciences Corp) surgically implanted subcutaneously and posteriorly to the interscapular brown adipose tissue (iBAT). Mice were anaesthetized with 2% isoflurane during surgery. Signals from G2 E-Mitters were detected by ER400 Energizer/Receivers (STARR Life Sciences Corp.) and data collection was integrated into the TSE software.

2.4. Glucose homeostasis assessments

Mice were subjected to a glucose tolerance test with 2 g/kg lean mass dextrose (D9434, Sigma-Aldrich) injected i.p. following a 6 h fast in clean cages. Blood glucose was measured from tail vein blood at baseline and at 15, 30, 60 and 120 min post-injection using Contour® Blood Glucose Meters and test strips (Bayer). The glucose tolerance test was performed at least one week before and after any other experiment to avoid interference of effects. Plasma insulin was measured using a kit (K152BZC, Mesoscale).

2.5. NAD^+ measurements

The assay was performed as previously described [29]. In short, 10—350 mg tissue was lysed in 400 µl 0.6 M perchloric acid. The supernatant was diluted 100-fold (iBAT) or 400-fold (eWAT and scWAT) in 100 mM Na_2HPO_4 (final pH 8.0), and NAD^+ was measured in 100 µl of the sample. 100 µl reaction mix (2% ethanol, 90 U/ml alcohol dehydrogenase, 130 mU/ml diaphorase, 10 µM resazurin, 10 µM flavin mononucleotide, 10 mM nicotinamide in phosphate buffer (200 mM Na_2HPO_4), pH 8.0) was added, and continuous resorufin accumulation was measured for 30 min by fluorescence excitation at 544 nm and emission at 580 nm.

2.6. Gene expression

Total RNA was extracted from tissue using TRI Reagent (T9424, Sigma-Aldrich) and subsequent isolation using RNeasy Mini Kit (74106, Qiagen). Reverse transcription was carried out on 500—1000 ng RNA using the High Capacity cDNA Reverse Transcription kit (4368814, Applied Biosystems). Gene expression was determined using SYBR green (PP00259, Primerdesign) based real-time quantitative PCR and normalization to the housekeeping gene *36b4*. Expression data were normalized to the mean of the control group. Primers are available in Supplemental Table 1.

2.7. Triglyceride assay

Serum triglycerides were determined using a kit (TR0100, Sigma-Aldrich). Tissue triglyceride content was determined by measuring glycerol content with Infinity TG Reagent (TR22421, Fischer Scientific) in saponified, neutralized tissue, achieved by incubating in ethanolic KOH overnight at 55°C and adding 0.5 M $MgCl_2$.
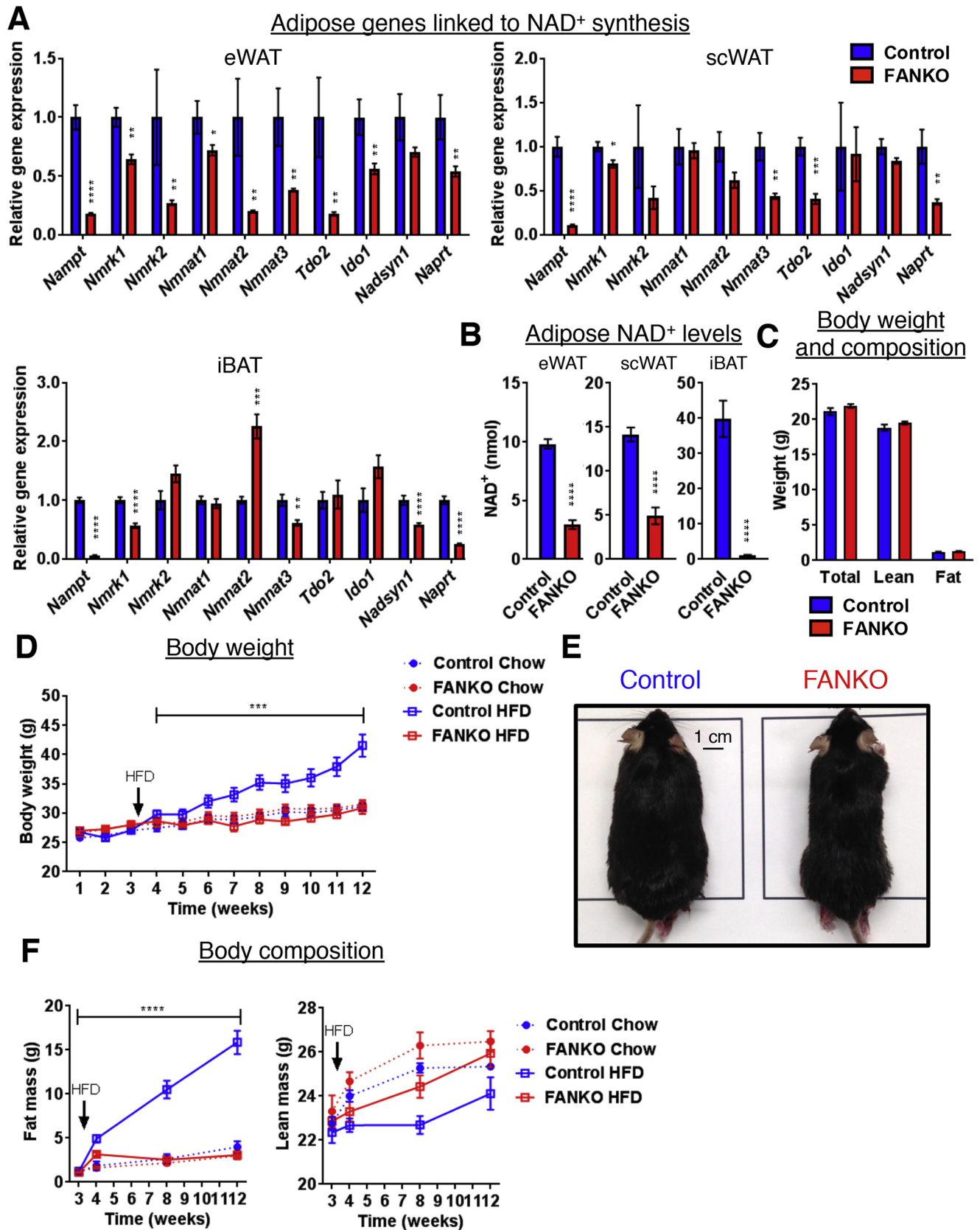
Figure 1: Adipose *Nampt* deficiency is protective against diet-induced obesity. Relative expression of NAD$^+$ biosynthesis genes (A) and whole tissue NAD$^+$ content (B) in eWAT, scWAT, and iBAT of male Nampt$^{f/f}$, Cre$^-$ (control) and FANKO mice on chow diet. (C) Body weight and composition of male control and FANKO mice on chow diet. Body weight (D), representative image (E) and body composition (F) of male control and FANKO mice fed a 60% HFD over 9 weeks. Data are expressed as mean ± SEM. *$p < 0.05$, **$p < 0.01$, ***$p < 0.001$, ****$p < 0.0001$ as determined by unpaired, two-tailed t-test and 2-way ANOVA (HFD-fed groups only).

2.8. Histology

5-10 mm tissue samples were fixed in 4% paraformaldehyde, dehydrated in ethanol and xylene, and embedded in paraffin. 4 μm tissue sections were deparaffinized, rehydrated, and stained using a standard Mayer's Haematoxylin and Eosin Y (H&E) or Sirius Red staining protocol. Histological images were acquired using light microscopy. Adipocyte area was measured using ImageJ software. Data were collected from 3 H&E-stained
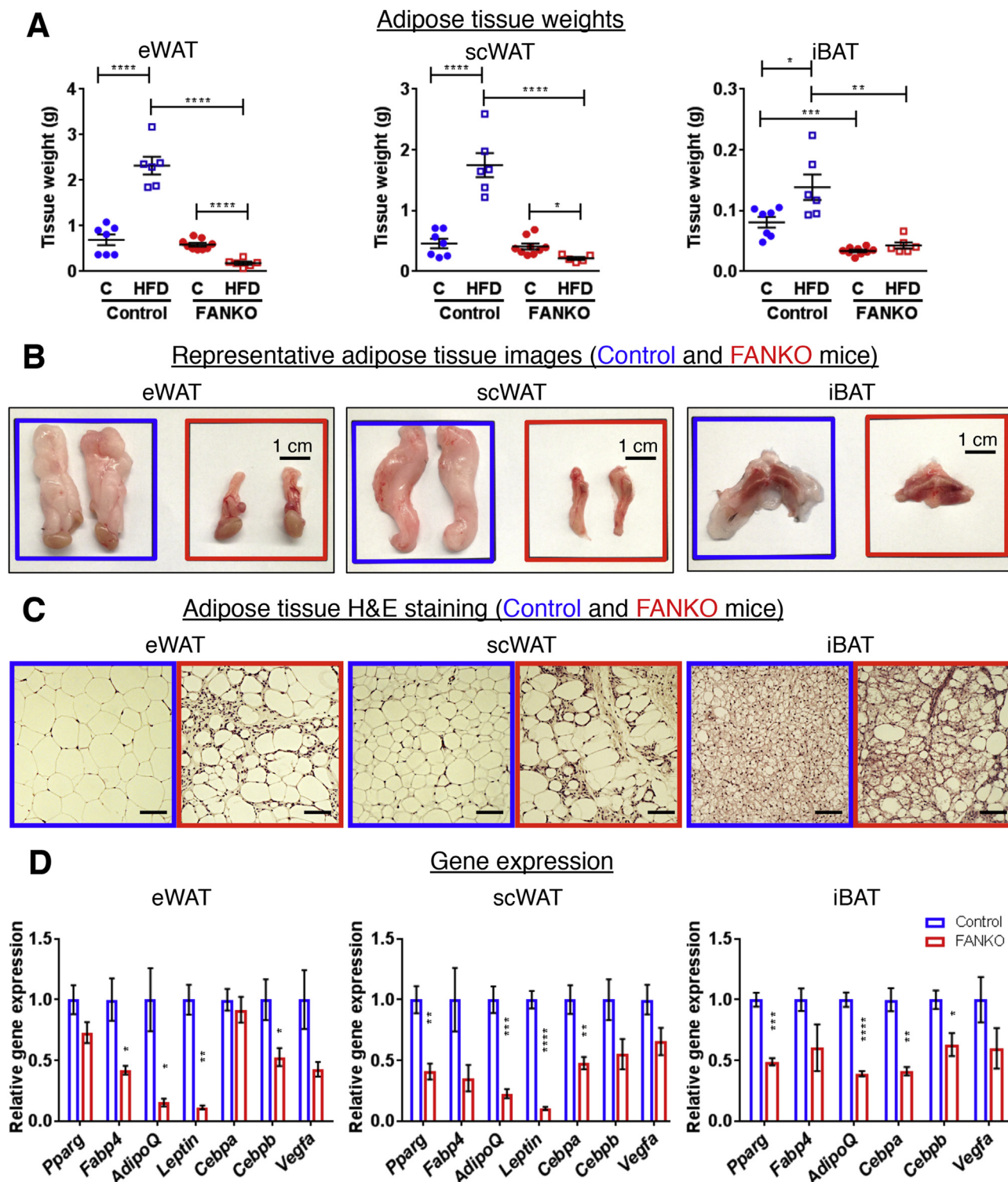

Figure 2: NAD$^+$ biosynthesis is crucial for adipose expansion from high dietary fat. (A) Weight of eWAT, scWAT, and iBAT of HFD and chow ("C") fed control and FANKO mice. (B) Pictures of eWAT (with testes), scWAT and iBAT (with surrounding white adipose tissue) of HFD-fed male mice and (C) H&E stained histological sections (Scale bar 100 μm). (D) Gene expression of eWAT, scWAT, and iBAT. Mice were on HFD for 11—16 weeks. Data are expressed as mean ± SEM. *$p < 0.05$, **$p < 0.01$, ***$p < 0.001$, ****$p < 0.0001$ as determined by unpaired, two-tailed t-test.
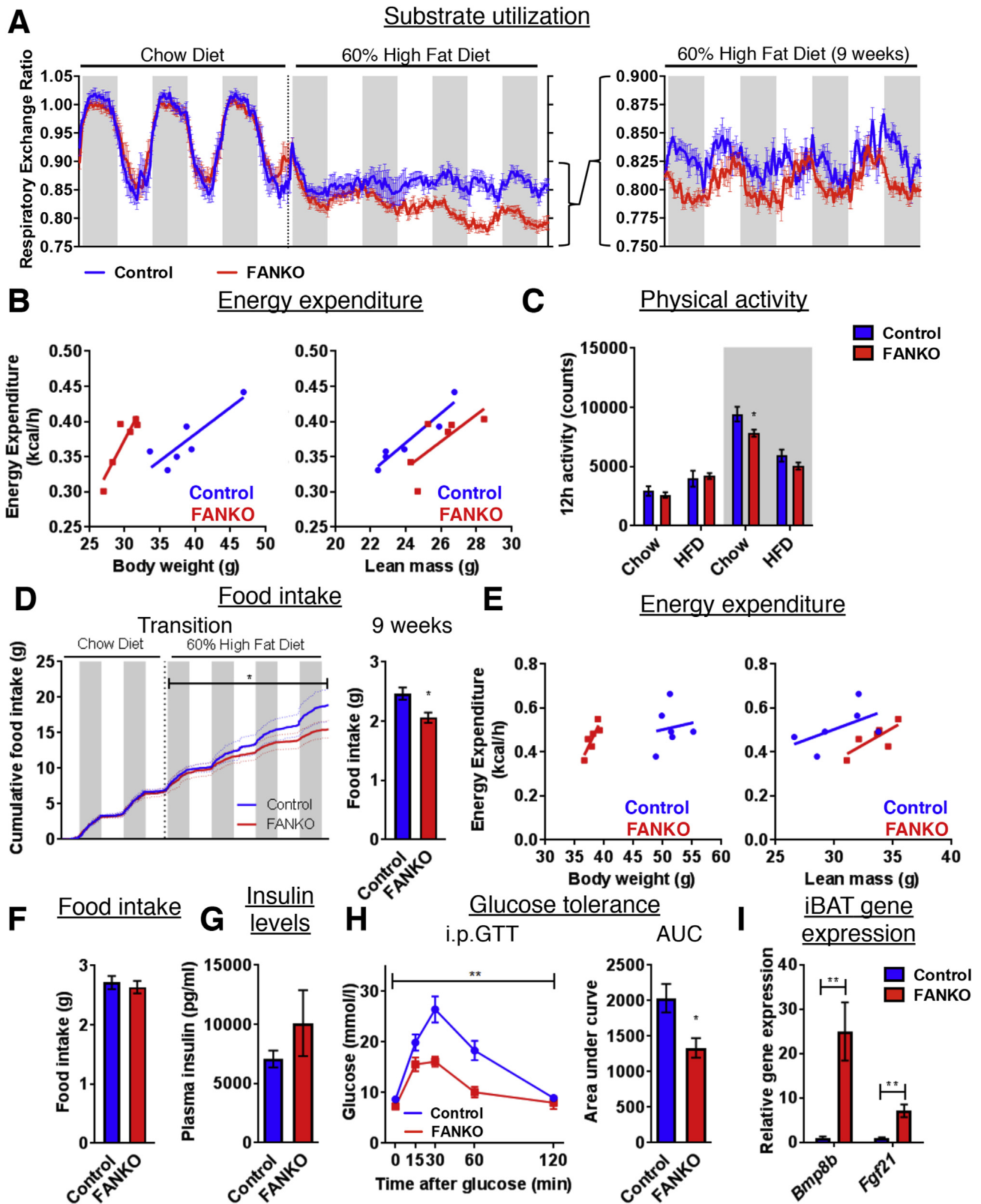
Figure 3: Loss of adipose *Nampt* decreases food intake and improves glucose tolerance. (A) Respiratory exchange ratio of male control and FANKO mice on regular chow diet and during transition to 60% HFD (left panel), and after 9 weeks on HFD (right panel). White areas represent the light phase (6am-6pm) and shaded areas represent the dark phase (6pm-6am). (B) Energy expenditure relative to body weight (left panel) and lean mass (right panel) after 9 weeks of HFD. (C) Physical activity during light (white) and dark phase (shaded) on chow or HFD. (D) Food intake on regular chow diet and during transition to 60% HFD (left panel) and after 9 weeks on HFD (right panel). White areas represent the light phase (6am-6pm), and shaded areas represent the dark phase (6pm-6am). (E) Energy expenditure relative to body weight (left panel) and lean mass (right panel), (F) food intake, (G) plasma insulin levels, (H) i.p. glucose tolerance test, and AUC, and (I) iBAT gene expression of secreted factors in male mice fed a HFD for 5−6 months. Data are expressed as mean $\pm$ SEM. *$p < 0.05$, **$p < 0.01$ as determined by unpaired, two-tailed t-test and 2-way ANOVA. In (D), statistical analysis was only performed after HFD introduction.
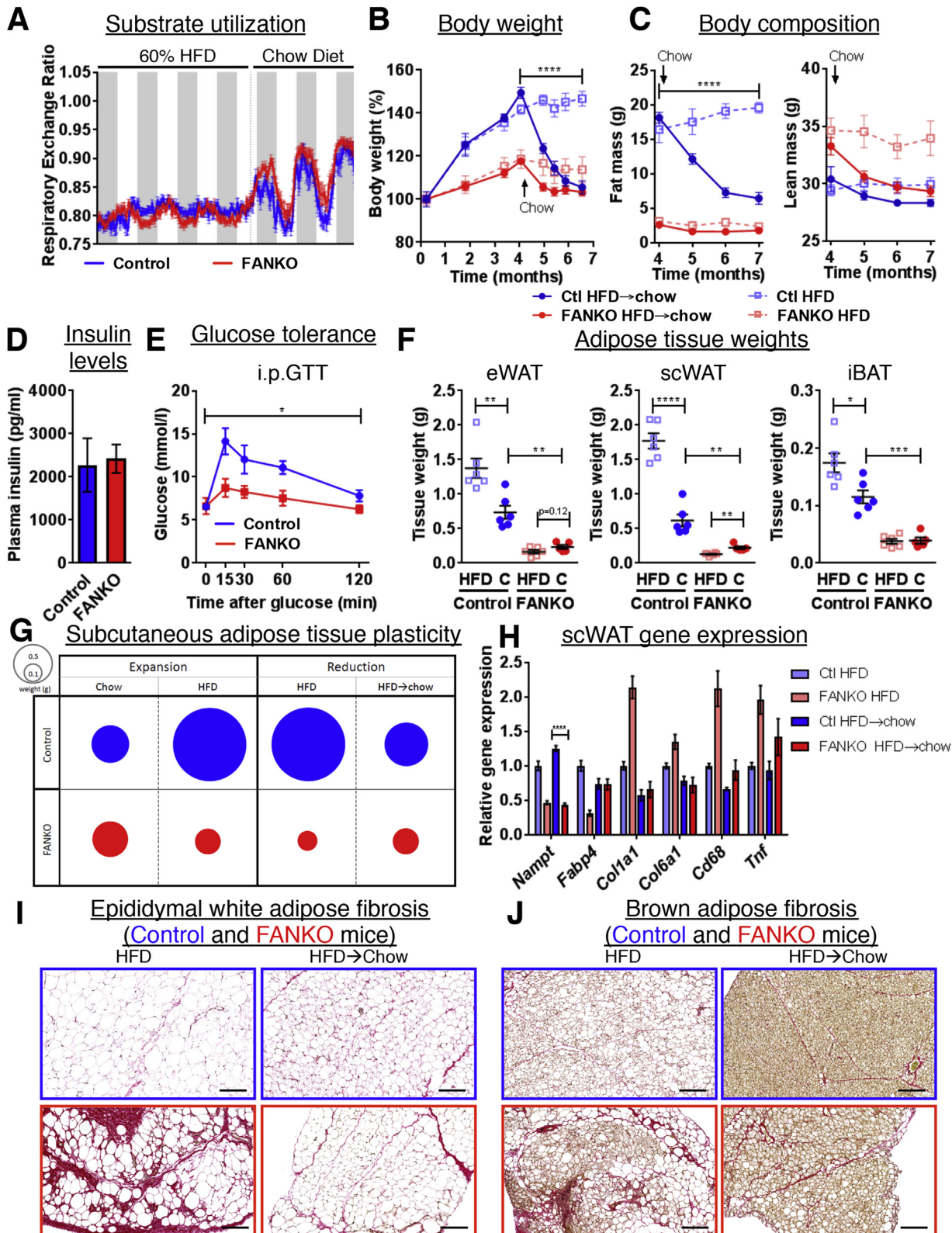
Figure 4: HFD-induced metabolic dysfunction in FANKO mice is reversible whereas improved glucose tolerance persists. (A) Respiratory exchange ratio (white areas represent the light phase (6am-6pm) and shaded areas represent the dark phase (6pm-6am)), (B) body weight, and (C) body composition (C) of HFD-fed male control and FANKO mice switched from HFD back to chow diet. (D) Plasma insulin levels and (E) i.p. GTT in male mice after 5 weeks back on chow. (F) Weight of eWAT, scWAT, and iBAT of male mice on HFD and switched back to chow ("C'") for 11 weeks. (G) Adipose plasticity of male FANKO mice. Area of the circle represents scWAT mean weight in the groups depicted in Figures 2A and 4F. (H) Gene expression of scWAT. Sirius red stain of eWAT (I) and iBAT (J) in male control and FANKO mice on HFD or switched back to chow for 11 weeks (Scale bar 200 μm). Data are expressed as mean ± SEM. *p < 0.05, **p < 0.01, ***p < 0.001, ****p < 0.0001 as determined by unpaired, two-tailed t-test and 2-way ANOVA. In (B), (C), and (H), statistical analyses were only performed on groups switched from HFD to chow diet. In (F), statistical analysis was not performed between the two HFD fed groups.

sections per mouse. Average of 150–200 cells per mouse is presented.

2.9. Mitochondrial respiration

Mitochondrial respiratory capacity was measured as described elsewhere [30]. Briefly, mitochondria were isolated from inter- and subscapular brown adipose tissues of chow fed mice using gradient centrifugation. Total protein content of the crude mitochondrial fraction was quantified using BCA assay (23225, ThermoFisher). 2 μg of mitochondria was loaded into each well of a Seahorse plate and spun down at 4 °C for 20 min at 2,000 g. The assay was conducted in a medium containing 125 mM sucrose, 20 mM K^+-TES (pH 7.2), 2 mM $MgCl_2$, 1 mM EDTA, 4 mM KH_2PO_4, and 0.1% fatty-acid-free BSA, with the indicated substrates and inhibitors.

2.10. Primary adipocytes

Primary preadipocytes were isolated from the stromal vascular fraction of iBAT and scWAT from 6-weeks-old male $Nampt^{f/f}$ mice with or without ROSA26-CreERT2. Cells were grown in DMEM (31966, Gibco) with 10% FBS (F7524, Sigma-Aldrich) and treated with 4-Hydroxytamoxifen (1 μM. H6278, Sigma-Aldrich) for two days before differentiation. Differentiation was induced by insulin (0.5 μg/ml. I9278, Sigma-Aldrich) dexamethasone (0.1 μM D4902, Sigma-Aldrich), rosiglitazone (1 μM. 71740-5, Cayman), T3 (1 nM. T6397, Sigma-Aldrich) and IBMX (250 μM. I5879, Sigma-Aldrich) for two days and maintained by insulin and T3 for five days until harvest on day 7.

2.11. Statistical analyses

Data are presented as mean ± SEM. Differences between two groups were evaluated using unpaired, two-tailed t-test. Variables over time were evaluated with two-way ANOVA. If all groups are not included in the statistical analyses, this is mentioned in the figure legends. GraphPad Prism version 7 was used for statistical analyses. $p < 0.05$ was considered statistically significant.

3. RESULTS

3.1. Adipose *Nampt* deficiency is protective against diet-induced obesity

To address the role of adipose NAMPT in the context of obesity, floxed *Nampt* mice [27] were bred to animals expressing Cre recombinase under the control of the adiponectin promoter [28] to produce fat-specific *Nampt* knockouts (FANKO). Targeted genetic deletion of *Nampt* led to statistically significant changes in the expression of several NAD^+ synthesis genes in adipose depots (Figure 1A). However, *Nampt* was unquestionably the most enriched among these enzymes suggesting a predominant role in adipose NAD^+ biosynthesis (Supplemental Figure 1A). Accordingly, NAD^+ levels were markedly reduced in all three adipose tissues from FANKO mice (Figure 1B).

We observed no change in body weight or fat and lean mass composition between FANKO and control mice maintained on a chow diet (Figure 1C). These results are in agreement with the previously published model of adipose *Nampt* loss-of-function in which exons 5–6 were deleted [15]. Moreover, *Nampt* deletion in preadipocytes did not impinge on adipocyte differentiation (Supplemental Figure 1B–C). Given the relatively low lipid content of the chow diet, this is also in line with our hypothesis that NAMPT primarily plays a role in efficient storage and handling of excess calories. To this end, we metabolically challenged FANKO mice and littermate controls with a diet in which 60% of the calories were derived from fat. FANKO mice were

completely resistant to HFD-induced obesity (Figure 1D–E). In fact, the pattern of weight gain for FANKO mice on HFD was virtually indistinguishable from that of chow-fed animals of either genotype. The striking weight difference between FANKO and control mice on HFD was entirely attributable to lipid accumulation (Figure 1F). By nine weeks of HFD, controls showed a 13-fold increase in fat mass whereas fat mass in FANKO mice was identical to chow-fed animals of either genotype. Weight gain in FANKO mice was predominantly driven by age-dependent increases in lean mass (Figure 1F). Together, these data indicate that NAMPT plays an essential and specific role in adipose by facilitating weight gain in response to dietary fat.

3.2. NAD^+ biosynthesis is crucial for adipose expansion from high dietary fat

We next investigated the biological consequences that challenging the fat-specific *Nampt* deletion with HFD imposed on the adipose tissue itself. In control mice, all fat pads were increased in size by HFD (Figure 2A). FANKO mice had slightly, but not significantly, increased iBAT size, whereas eWAT and scWAT weights were surprisingly decreased upon high fat feeding (Figure 2A). Images from representative HFD-fed FANKO and control mice depict striking differences in eWAT and scWAT size, whereas iBAT, apart from a reduction in the amount of surrounding white adipose, did not appear dramatically altered (Figure 2B). However, histological analysis revealed aberrations in all three depots (Figure 2C). White fat pads from FANKO mice exhibited massive fibrosis (Figure 2C), infiltration by non-adipocyte species (Figure 2C), and reduction in average lipid droplet size (Supplemental Figure 2A). A similar fibrotic phenotype was observed in FANKO iBAT (Figure 2C). Brown adipocytes from these mice appeared larger and possessed more unilocular lipid droplets compared to adipocytes from HFD-fed controls (Figure 2C). Adipocyte markers were markedly reduced in all three depots (Figure 2D), indicating compromised adipocyte integrity and/or appropriation by non-adipocyte species. Adipose tissue function is highly dependent on proper oxygen availability [31] that can be approximated through the level of angiogenesis. Expression of the key angiogenic growth factor *Vegfa* was reduced, though not significantly, in both white and brown adipose from FANKO mice, suggesting compromised vascularization (Figure 2D).

When adipose depots are unable to accommodate the burden from high dietary fat consumption, excess lipids are often pathologically redistributed to other organs, most notably the liver. Accordingly, we found that livers of FANKO mice were larger (Supplemental Figure 2B–C) and more enriched in triglycerides (TGs) compared to those of controls (Supplemental Figure 2D). However, interestingly, FANKO mice had reduced TG levels in both quadriceps and gastrocnemius (Supplemental Figure 2E) and plasma TGs were unaffected (Supplemental Figure 2F). Together, these data indicate that NAD^+ biosynthesis in adipocytes is critical for physiological expansion of white adipose depots in response to high dietary fat and may play a more specific role in lipid handling and accumulation. In the absence of NAMPT, adipocytes are unable to cope with the metabolic burden resulting in tissue dysfunction and ectopic lipid deposition in liver but not skeletal muscle.

3.3. Loss of adipose *Nampt* decreases food intake and improves glucose tolerance

Severe disruptions in adipocyte biology, including excessive accumulation of extracellular matrix, can lead to dramatic alterations in systemic energy homeostasis [6,32,33]. To address the systemic ramifications of fat-specific *Nampt* deletion, we

performed indirect calorimetry on FANKO mice and control litter-mates under chow-fed conditions and at various stages of a HFD challenge. We assessed carbohydrate versus lipid substrate utilization by calculating the respiratory exchange ratio (RER) and observed no genotypic differences in daily RER oscillations in mice on chow diet (Figure 3A, left panel). However, upon initiation of the HFD, control animals developed an arrhythmic RER, consistent with previous work on HFD-induced disruption of circadian physiology [34]. Intriguingly, FANKO mice transitioned to HFD gradually adopted a sustained RER biorhythm that was completely inverted compared to the pattern seen in chow-fed mice of either genotype (Figure 3A).

To gain insight into how FANKO mice were protected from diet-induced obesity, we measured energy expenditure, physical activity, food intake, and body temperature in animals on HFD. FANKO mice exhibited increased energy expenditure when adjusted to body weight (Figure 3B, left panel). However, given the large disparity in body composition between the genotypes, the less metabolically active fat mass of control mice may account for at least some of this difference [35]. Accordingly, when adjusted to lean mass (Figure 3B, right panel), FANKO mice had unchanged or slightly decreased energy expenditure. In agreement with this observation, physical activity was genotypically-similar on HFD: whereas chow-fed FANKO mice displayed less physical activity than controls during the dark (i.e. active) phase, as previously observed in another adipose *Nampt* deficiency model [15], this difference was diminished after animals were transitioned to HFD (Figure 3C).

To directly assess the contribution of brown adipose energy dissipation in FANKO mice, we measured UCP1-dependent respiration of iBAT mitochondria in response to several different substrates. Loss of *Nampt* dramatically attenuated mitochondrial respiration induced by malate/pyruvate, glycerol-3-phosphate, and succinate (Supplemental Figure 3A). Despite the thermogenically inactive mitochondria in iBAT, FANKO mice maintained body temperature on both chow and HFD (Supplemental Figure 3B). Whether there are compensatory temperature defense mechanisms induced to account for FANKO iBAT dysfunction is not clear. However, such compensation is unlikely to originate from oxygen-consuming fat free mass (Figure 3B, right panel). Together, these data suggest that the profound difference in HFD-induced adiposity between FANKO mice and control littermates was not directly attributable to adipose or lean mass-driven energy expenditure. Given that energy output did not seem to be a primary driver of the weight phenotype, we next examined food intake. We observed no difference in mice on chow diet. However, upon transitioning to HFD, FANKO mice immediately reduced their food intake relative to controls (Figure 3D, left panel), and it remained consistently lower in FANKO mice after 9 weeks on HFD (Figure 3D, right panel). This reduction was likely not driven by increased leptin signaling, as leptin expression was reduced in white adipose depots (Figure 2D). Therefore, the striking body weight difference in HFD-fed FANKO mice seems to be at least partially attributable to the combination of reduced food intake and the inability of adipose to accumulate lipid (Figure 2).

We further examined FANKO mice and control littermates in the context of a chronic HFD challenge over 5−6 months. Energy expenditure exhibited a similar pattern as during the short-term HFD and appeared to be increased when adjusted for total body weight (Figure 3E, left panel). However, when corrected by lean mass, FANKO energy expenditure again remained slightly reduced relative to control litter-mates (Figure 3E, right panel). Interestingly, food intake was now equal between the two genotypes (Figure 3F), likely indicating that both groups had reached a metabolic steady state compared to the more

acute HFD challenge. Given that adipose dysfunction is often followed by disturbances in glucose homeostasis [33,36,37], we assessed glycemic control in HFD-fed FANKO mice. Fasting serum insulin levels were equal between the two genotypes (Figure 3G) but, surprisingly, FANKO mice were remarkably more glucose tolerant (Figure 3H). To avoid confounding factors from the divergent fat masses, the dose of the glucose bolus administered was based on lean mass, which was comparable between genotypes.

How FANKO mice were significantly more glucose tolerant than controls was not clear. Due to the reduced mitochondrial capacity of FANKO iBAT and the atrophied, fibrotic nature of white depots in FANKO mice, adipose tissue seemed unlikely as the tissue accountable for increased glucose uptake. However, we speculated that adipose tissue could be indirectly responsible by inducing expression of BAT secreted factors linked to systemic glucose homeostasis. Indeed, two such factors, bone morphogenetic protein 8b (*Bmp8b*) and fibroblast growth factor 21 (*Fgf21*) [38,39], were significantly higher expressed in FANKO iBAT compared to controls (Figure 3I). We hypothesize that FANKO-mediated defects in adipose during a HFD challenge triggered the release of soluble factors in an attempt to mitigate systemic metabolic dysfunction. Skeletal muscle seems a viable candidate for contributing to the elevated glucose tolerance particularly given the significantly lower triglyceride content in the FANKO muscles analyzed (Supplemental Figure 2E). Nevertheless, our findings reveal that loss of adipose NAMPT profoundly alters the systemic response to high dietary fat intake by reprogramming patterns of substrate utilization, decreasing food intake, and improving glycemic control.

3.4. HFD-induced metabolic dysfunction in FANKO mice is reversible whereas improved glucose tolerance persists

Healthy adipose tissue displays a robust plasticity to expand and contract in both number and size of adipocytes depending on nutrient availability [5,6]. To address the role of NAMPT in adipose plasticity, we transitioned FANKO mice and control littermates back to chow diet after four months of HFD feeding. Strikingly, after only one day on chow diet, control animals re-established a synchronous RER oscillation reminiscent of the RER of chow-fed mice (Figure 4A). Moreover, in the same time span, FANKO mice shifted to a similar RER rhythm, completely reversing the HFD-induced inverted pattern. The difference in amplitude of the RER biorhythm between controls and FANKO mice was likely attributable to the starkly contrasting size of adipose depots and thus substrate availability.

Throughout the course of the dietary switch, both genotypes displayed weight loss that ultimately plateaued 11 weeks after shifting to chow diet (Figure 4B). However, control mice still retained higher fat mass and slightly lower lean mass than FANKO animals (Figure 4C). Analogous to the chronic HFD challenge, FANKO mice switched back to chow diet maintained similar insulin levels (Figure 4D), significantly higher glucose tolerance (Figure 4E and Supplemental Figure 4A), and elevated *Fgf21* and *Bmp8b* expression levels (Supplemental Figure 4B) compared to control littermates. Consistent with the MR data, fat depots from control mice were all significantly reduced following the switch from HFD back to chow diet (Figure 4F). Conversely, in FANKO mice scWAT significantly increased in size and eWAT showed a tendency towards increasing (Figure 4F) suggesting that NAMPT-deficient adipose was able to re-establish lipid storage once the burden of high dietary fat was alleviated. Graphical depiction of white adipose weights from HFD challenge and transition back to chow illustrates the pivotal role that NAD$^+$ biosynthesis plays in adipose expansion and contraction (Figure 4G and Supplemental Figure 4C). Moreover, transitioning animals from HFD back to chow resulted in a normalization of *Fabp4*

and collagen expression, as well as a partial macrophage and cytokine normalization in scWAT (Figure 4H). These findings are consistent with our results in primary adipocytes in which *Nampt* depletion had little effect on differentiation capacity (Supplemental Figure 1B—C). Histologically, we observed marked reversal of fibrosis in white fat depots from FANKO mice (Figure 4I and Supplemental Figure 4D). Multilocular lipid storage in FANKO iBAT was partially restored (Figure 4J). Furthermore, liver weights and TG concentrations of both control and FANKO mice were indistinguishable after transitioning from HFD back to chow (Supplemental Figure 4E—F). Taken together, these observations establish the critical importance of NAMPT for adipose plasticity in specifically handling dietary fat.

4. DISCUSSION

Given the integral role of NAD^+ in cellular metabolism, it is surprising that adipose NAD^+ depletion in FANKO mice, as well as in a previous *Nampt* loss-of-function model [15], does not produce more severe ramifications on adipose biology, fat mass, or body weight. However, the lower fat concentration of standard murine chow diet may offer an explanation. In this nutrient state, the primary function of adipose tissue, energy storage, is not particularly challenged. This is analogous to studying liver and skeletal muscle metabolism in the absence of feeding/fasting or exercise regiments, respectively. Accordingly, when mice were subjected to the stress of a diet rich in fat, animals lacking NAMPT-mediated NAD^+ salvage were unable to handle the lipid burden. The specificity of this lipid-handling requirement was further underscored when the HFD burden was alleviated and adipose dysfunction in FANKO mice was largely reversed. In the context of evolution, we believe adipose NAMPT would have been highly advantageous for efficiently accumulating fat mass from dietary fat. However, as evidenced by the significant association between *NAMPT* and obesity in humans [18—21], this program may now be a liability with modern lipid-laden diets.

The complete prevention of diet-induced obesity in FANKO mice certainly raises the provocative notion that NAMPT inhibitors could be explored as a pharmacological avenue for weight reduction. Indeed, NAMPT inhibitors have already been investigated for treatment of several forms of cancer [40]. However, in light of the detrimental impact of NAD^+ depletion on adipose tissue during a HFD challenge and the central role of NAD^+/NADH metabolism [41], direct NAMPT inhibition does not pose a viable therapeutic option for obesity. Moreover, NAMPT is expressed across numerous organ systems in which it plays critical roles in tissue-specific metabolism. For example, loss of NAD^+ biosynthesis in skeletal muscle impairs mitochondrial function, is degenerative, and diminishes exercise capacity [27,42], whereas overexpression of *Nampt* in skeletal muscle confers partial protection from ageing-associated [42] and HFD-induced [43] weight gain. Nevertheless, future studies identifying how adipose *Nampt* deficiency triggers reduced food intake and increased glucose tolerance could lead to a more targeted, clinically appealing approach. Based on our data, one strong possibility is a secreted factor or factors from NAD^+-depleted adipocytes that is meant to counteract the adipose dysfunction in FANKO mice. In this study, we focused on the expression of factors from brown adipocytes; however, we cannot rule out white adipocytes or pre-adipocytes as a source [44]. Such factors, originating from adipose, could potentially be developed into a novel treatment strategy to facilitate dietary and glycemic control without the deleterious effects of *Nampt* deficiency.

Our study raises a number of additional questions requiring further investigation. Why is food intake only reduced in FANKO mice upon transitioning to HFD? Injection of eNAMPT into hypothalami of rats has previously been shown to increase food intake in rats [45]. However, these experiments were performed in the setting of a chow-like diet [45] and male adipose *Nampt* KO mice do not have different eNAMPT levels compared to controls [15]. Together with our data, this implies the existence of an additional factor or mechanism of modulating food intake that is specific to high dietary fat. It is tempting to speculate that adipose NAMPT is part of a control system designed to regulate dietary fat intake based on storage capacity. If the dysfunctional adipose tissue in HFD-fed FANKO mice is indeed secreting such a signaling factor, an equally pressing question is what tissues are receiving the signal to increase glucose uptake? The tissue responsible for increased glucose tolerance could be ascertained by measuring 2-deoxyglucose uptake *in vivo*. Furthermore, can the ability of FANKO mice to store dietary fat be rescued by supplementation with NAD^+ precursors like nicotinamide mononucleotide (NMN) [15] or nicotinamide riboside (NR) [46] as has been done in other contexts?

As the current study focuses exclusively on male mice, it does not clarify whether there are sex-specific differences in the handling of adipose NAD^+ depletion in the context of high fat feeding. Still, it is well established that adipose tissue biology varies between sexes [47,48] including the release of secreted factors from the FGF and BMP families [49]. Moreover, in an earlier model of adipose *Nampt* deficiency chow-fed female mice were found to be glucose intolerant whereas male adipose *Nampt* knockouts were indistinguishable from controls [17], indicating that FANKO mice may also handle HFD in a sex-specific manner. One final consideration is that our FANKO model depletes NAD^+ uniformly across all adipose depots. What is the contribution of NAMPT function in white versus brown fat tissues to our observed phenotypes? A brown and beige fat loss-of-function model using the *Ucp1*-Cre model [50] would be necessary for making this distinction. Nonetheless, our findings here establish the unequivocal necessity of NAMPT for adipose plasticity specifically in the context of high dietary fat.

CONFLICT OF INTEREST

None declared.

APPENDIX A. SUPPLEMENTARY DATA

Supplementary data related to this article can be found at https://doi.org/10.1016/j.molmet.2018.02.014.

DECLARATION OF INTEREST

The authors have no conflicts of interest.

REFERENCES

[1] Brown, P.J., 1991. Culture and the evolution of obesity. Hawthorne, N.Y.: Human Nature. p. 31–57. https://doi.org/10.1007/BF02692180, 2(1).

[2] Bellisari, A., 2008. Evolutionary origins of obesity. Obesity Reviews: An Official Journal of the International Association for the Study of Obesity 9(2):165–180. https://doi.org/10.1111/j.1467-789X.2007.00392.x.

[3] Gerhart-Hines, Z., Lazar, M.A., 2015. Circadian metabolism in the light of evolution. Endocrine Reviews 36(3):289–304. https://doi.org/10.1210/er.2015-1007.

[4] Smorlesi, A., Frontini, A., Giordano, A., Cinti, S., 2012. The adipose organ: white-brown adipocyte plasticity and metabolic inflammation: adipocyte plasticity and adipose organ. Obesity Reviews 13:83–96. https://doi.org/10.1111/j.1467-789X.2012.01039.x.

[5] Pellegrinelli, V., Carobbio, S., Vidal-Puig, A., 2016. Adipose tissue plasticity: how fat depots respond differently to pathophysiological cues. Diabetologia 59(6):1075–1088. https://doi.org/10.1007/s00125-016-3933-4.

[6] Sun, K., Kusminski, C.M., Scherer, P.E., 2011. Adipose tissue remodeling and obesity. Journal of Clinical Investigation 121(6):2094–2101. https://doi.org/10.1172/JCI45887.

[7] Wang, Q.A., Tao, C., Gupta, R.K., Scherer, P.E., 2013. Tracking adipogenesis during white adipose tissue development, expansion and regeneration. Nature Medicine 19(10):1338–1344. https://doi.org/10.1038/nm.3324.

[8] Grandl, G., Müller, S., Moest, H., Moser, C., Wollscheid, B., Wolfrum, C., 2016. Depot specific differences in the adipogenic potential of precursors are mediated by collagenous extracellular matrix and Flotillin 2 dependent signaling. Molecular Metabolism 5(10):937–947. https://doi.org/10.1016/j.molmet.2016.07.008.

[9] Zhou, Y.T., Wang, Z.W., Higa, M., Newgard, C.B., Unger, R.H., 1999. Reversing adipocyte differentiation: implications for treatment of obesity. Proceedings of the National Academy of Sciences of the United States of America 96(5): 2391–2395.

[10] Yoshino, J., Mills, K.F., Yoon, M.J., Imai, S.I., 2011. Nicotinamide mononucleotide, a key NAD(+) intermediate, treats the pathophysiology of diet- and age-induced diabetes in mice. Cell Metabolism 14(4):528–536. https://doi.org/10.1016/j.cmet.2011.08.014.

[11] Chalkiadaki, A., Guarente, L., 2012. High-fat diet triggers inflammation-induced cleavage of SIRT1 in adipose tissue to promote metabolic dysfunction. Cell Metabolism 16(2):180–188. https://doi.org/10.1016/j.cmet.2012.07.003.

[12] Miller, K.N., Burhans, M.S., Clark, J.P., Howell, P.R., Polewski, M.A., DeMuth, T.M., et al., 2017. Aging and caloric restriction impact adipose tissue, adiponectin, and circulating lipids. Aging Cell 16(3):497–507. https://doi.org/10.1111/acel.12575.

[13] Song, J., Ke, S.F., Zhou, C.C., Zhang, S.L., Guan, Y.F., Xu, T.Y., et al., 2014. Nicotinamide phosphoribosyltransferase is required for the calorie restriction-mediated improvements in oxidative stress, mitochondrial biogenesis, and metabolic adaptation. Journals of Gerontology - Series A Biological Sciences and Medical Sciences 69(1):44–57. https://doi.org/10.1093/gerona/glt122.

[14] Revollo, J.R., Grimm, A.A., Imai, S., 2004. The NAD biosynthesis pathway mediated by nicotinamide phosphoribosyltransferase regulates Sir2 activity in mammalian cells. The Journal of Biological Chemistry 279(49):50754–50763. https://doi.org/10.1074/jbc.M408388200.

[15] Yoon, M.J.J., Yoshida, M., Johnson, S., Takikawa, A., Usui, I., Tobe, K., et al., 2015. SIRT1-Mediated eNAMPT secretion from adipose tissue regulates hypothalamic NAD+ and function in mice. Cell Metabolism 21(5):706–717. https://doi.org/10.1016/j.cmet.2015.04.002.

[16] Revollo, J.R., Körner, A., Mills, K.F., Satoh, A., Wang, T., Garten, A., et al., 2007. Nampt/PBEF/visfatin regulates insulin secretion in β cells as a systemic NAD biosynthetic enzyme. Cell Metabolism 6(5):363–375.

[17] Stromsdorfer, K.L., Yamaguchi, S., Yoon, M.J., Moseley, A.C., Franczyk, M.P., Kelly, S.C., et al., 2016. NAMPT-mediated NAD+ biosynthesis in adipocytes regulates adipose tissue function and multi-organ insulin sensitivity in mice. Cell Reports, 1–10. https://doi.org/10.1016/j.celrep.2016.07.027.

[18] Berndt, J., Kloting, N., Kralisch, S., Kovacs, P., Fasshauer, M., Schon, M.R., et al., 2005. Plasma visfatin concentrations and fat depot-specific mRNA expression in humans. Diabetes 54(10):2911–2916. https://doi.org/10.2337/diabetes.54.10.2911.

[19] Garten, A., Schuster, S., Penke, M., Gorski, T., de Giorgis, T., Kiess, W., 2015. Physiological and pathophysiological roles of NAMPT and NAD metabolism. Nature Reviews Endocrinology 11(9):1–12. https://doi.org/10.1038/nrendo.2015.117.

[20] Terra, X., Auguet, T., Quesada, I., Aguilar, C., Luna, A.M., Hernández, M., et al., 2012. Increased levels and adipose tissue expression of visfatin in morbidly obese women: the relationship with pro-inflammatory cytokines. Clinical Endocrinology 77(5):691–698. https://doi.org/10.1111/j.1365-2265.2011.04327.x.

[21] Varma, V., Yao-Borengasser, A., Rasouli, N., Bodles, A.M., Phananavanh, B., Lee, M.-J., et al., 2007. Human visfatin expression: relationship to insulin sensitivity, intramyocellular lipids, and inflammation. The Journal of Clinical Endocrinology & Metabolism 92(2):666–672. https://doi.org/10.1210/jc.2006-1303.

[22] Barth, S., Klein, P., Horbach, T., Dötsch, J., Rauh, M., Rascher, W., et al., 2010. Expression of neuropeptide Y, omentin and visfatin in visceral and subcutaneous adipose tissues in humans: relation to endocrine and clinical parameters. Obesity Facts 3(4):245–251. https://doi.org/10.1159/000319508.

[23] Jukarainen, S., Heinonen, S., Rämö, J.T., Rinnankoski-Tuikka, R., Rappou, E., Tummers, M., et al., 2016. Obesity is associated with low NAD(+)/SIRT pathway expression in adipose tissue of BMI-Discordant monozygotic twins. The Journal of Clinical Endocrinology and Metabolism 101(1):275–283. https://doi.org/10.1210/jc.2015-3095.

[24] Rappou, E., Jukarainen, S., Rinnankoski-Tuikka, R., Kaye, S., Heinonen, S., Hakkarainen, A., et al., 2016. Weight loss is associated with increased NAD+/SIRT1 expression but reduced PARP activity in white adipose tissue. Journal of Clinical Endocrinology and Metabolism 101(3):1263–1273. https://doi.org/10.1210/jc.2015-3054.

[25] Tabassum, R., Mahendran, Y., Dwivedi, O.P., Chauhan, G., Ghosh, S., Marwaha, R.K., et al., 2012. Common variants of IL6, LEPR, and PBEF1 are associated with obesity in indian children. Diabetes 61(3):626–631. https://doi.org/10.2337/db11-1501.

[26] Blakemore, A.I.F., Meyre, D., Delplanque, J., Vatin, V., Lecoeur, C., Marre, M., et al., 2009. A rare variant in the visfatin gene (NAMPT/PBEF1) is associated with protection from obesity. Obesity (Silver Spring, Md.) 17(8):1549–1553. https://doi.org/10.1038/oby.2009.75.

[27] Agerholm, M., Dall, M., Jensen, B.A.H., Prats, C., Madsen, S., Basse, A.L., et al., 2017. Perturbations of NAD salvage systems impact mitochondrial function and energy homeostasis in mouse myoblasts and intact skeletal muscle. American Journal of Physiology - Endocrinology And Metabolism. https://doi.org/10.1152/ajpendo.00213.2017 ajpendo.00213.2017.

[28] Eguchi, J., Wang, X., Yu, S., Kershaw, E.E., Chiu, P.C., Dushay, J., et al., 2011. Transcriptional control of adipose lipid handling by IRF4. Cell Metabolism 13(3):249–259. https://doi.org/10.1016/j.cmet.2011.02.005.

[29] Dall, M., Penke, M., Sulek, K., Matz-Soja, M., Holst, B., Garten, A., et al., 2018. Hepatic NAD+levels and NAMPT abundance are unaffected during prolonged high-fat diet consumption in C57BL/6JBomTac mice. Molecular and Cellular Endocrinology. https://doi.org/10.1016/j.mce.2018.01.025.

[30] Shabalina, I.G., Jacobsson, A., Cannon, B., Nedergaard, J., 2004. Native UCP1 displays simple competitive kinetics between the regulators purine nucleotides and fatty acids. Journal of Biological Chemistry 279(37):38236–38248. https://doi.org/10.1074/jbc.M402375200.

[31] Trayhurn, P., 2013. Hypoxia and adipose tissue function and dysfunction in obesity. Physiological Reviews 93(1):1–21. https://doi.org/10.1152/physrev.00017.2012.

[32] Kusminski, C.M., Scherer, P.E., 2012. Mitochondrial dysfunction in white adipose tissue. Trends in Endocrinology and Metabolism: TEM 23(9):435–443. https://doi.org/10.1016/j.tem.2012.06.004.

[33] Danforth, E., 2000. Failure of adipocyte differentiation causes type II diabetes mellitus? Nature Genetics 26(1):13 https://doi.org/10.1038/79111.

[34] Kohsaka, A., Laposky, A.D., Ramsey, K.M., Estrada, C., Joshu, C., Kobayashi, Y., et al., 2007. High-fat diet disrupts behavioral and molecular circadian rhythms in mice. Cell Metabolism 6(11):414–421. https://doi.org/10.1016/j.cmet.2007.09.006.

[35] Tschöp, M.H., Speakman, J.R., Arch, J.R.S., Auwerx, J., Brüning, J.C., Chan, L., et al., 2012. A guide to analysis of mouse energy metabolism. Nature Methods 9(1):57–63. https://doi.org/10.1038/nmeth.1806.

[36] Rosen, E.D., Spiegelman, B.M., 2006. Adipocytes as regulators of energy balance and glucose homeostasis. Nature 444(7121):847–853. https://doi.org/10.1038/nature05483.

[37] Guilherme, A., Virbasius, J.V., Puri, V., Czech, M.P., 2008. Adipocyte dysfunctions linking obesity to insulin resistance and type 2 diabetes. Nature Reviews Molecular Cell Biology 9(5):367–377. https://doi.org/10.1038/nrm2391.

[38] Villarroya, F., Cereijo, R., Villarroya, J., Giralt, M., 2016. Brown adipose tissue as a secretory organ. Nature Reviews Endocrinology 13(1):26–35. https://doi.org/10.1038/nrendo.2016.136.

[39] Whittle, A.J., Carobbio, S., Martins, L., Slawik, M., Hondares, E., Vázquez, M.J., et al., 2012. BMP8B increases Brown adipose tissue thermogenesis through both central and peripheral actions. Cell 149(4):871–885. https://doi.org/10.1016/j.cell.2012.02.066.

[40] Sampath, D., Zabka, T.S., Misner, D.L., O'Brien, T., Dragovich, P.S., 2015. Inhibition of nicotinamide phosphoribosyltransferase (NAMPT) as a therapeutic strategy in cancer. Pharmacology and Therapeutics 151:16–31. https://doi.org/10.1016/j.pharmthera.2015.02.004.

[41] Cantó, C., Menzies, K.J., Auwerx, J., 2015. NAD(+) metabolism and the control of energy homeostasis: a balancing act between mitochondria and the nucleus. Cell Metabolism 22(1):31–53. https://doi.org/10.1016/j.cmet.2015.05.023.

[42] Frederick, D.W., Loro, E., Liu, L., Davila, A., Chellappa, K., Silverman, I.M., et al., 2016. Loss of NAD homeostasis leads to progressive and reversible degeneration of skeletal muscle. Cell Metabolism 24(2):269–282. https://doi.org/10.1016/j.cmet.2016.07.005.

[43] Costford, S.R., Brouwers, B., Hopf, M.E., Sparks, L.M., Dispagna, M., Gomes, A.P., et al., 2017. Skeletal muscle overexpression of nicotinamide phosphoribosyl transferase in mice coupled with voluntary exercise augments exercise endurance. Molecular Metabolism, 1–11. https://doi.org/10.1016/j.molmet.2017.10.012.

[44] Challa, T.D., Straub, L.G., Balaz, M., Kiehlmann, E., Donze, O., Rudofsky, G., et al., 2015. Regulation of De Novo adipocyte differentiation through cross talk between adipocytes and preadipocytes. Diabetes 64(12):4075–4087. https://doi.org/10.2337/db14-1932.

[45] Brunetti, L., Recinella, L., Di Nisio, C., Chiavaroli, A., Leone, S., Ferrante, C., et al., 2012. Effects of visfatin/PBEF/NAMPT on feeding behaviour and hypothalamic neuromodulators in the rat. Journal of Biological Regulators and Homeostatic Agents 26(2):295–302.

[46] Cantó, C., Houtkooper, R.H., Pirinen, E., Youn, D.Y., Oosterveer, M.H., Cen, Y., et al., 2012. The NAD+ precursor nicotinamide riboside enhances oxidative metabolism and protects against high-fat diet-induced obesity. Cell Metabolism 15(6):838–847. https://doi.org/10.1016/j.cmet.2012.04.022.

[47] Fuente-Martín, E., Argente-Arizón, P., Ros, P., Argente, J., Chowen, J.A., 2013. Sex differences in adipose tissue: it is not only a question of quantity and distribution. Adipocyte 2(3):128–134. https://doi.org/10.4161/adip.24075.

[48] Valencak, T.G., Osterrieder, A., Schulz, T.J., 2017. Sex matters: the effects of biological sex on adipose tissue biology and energy metabolism. Redox Biology 12:806–813. https://doi.org/10.1016/j.redox.2017.04.012.

[49] Grefhorst, A., van den Beukel, J.C., van Houten, E.L.A., Steenbergen, J., Visser, J.A., Themmen, A.P., 2015. Estrogens increase expression of bone morphogenetic protein 8b in brown adipose tissue of mice. Biology of Sex Differences 6(1). https://doi.org/10.1186/s13293-015-0025-y.

[50] Kong, X., Banks, A., Liu, T., Kazak, L., Rao, R.R., Cohen, P., et al., 2014. IRF4 is a key thermogenic transcriptional partner of PGC-1α. Cell 158(1):69–83 https://doi.org/10.1016/j.cell.2014.04.049.